

DEVELOPMENTS IN PERMEABILITY ENHANCEMENT FOR IN-SITU RECOVERY

By

Laura Kuhar

CSIRO Mineral Resources, Australia

Presenter and Corresponding Author

Laura Kuhar
laura.kuhar@csiro.au

ABSTRACT

In-situ recovery (ISR) has the potential to unlock mining opportunities in deposits that may otherwise be uneconomical to process by conventional means. Three critical components for the successful implementation of ISR include: (i) containment and hydrogeological control; the lixiviant must flow within the region of interest and be retained within this region, for economic and environmental reasons. (ii) Minerals of value must be exposed and leachable with the lixiviant system having good in-situ chemistry; the chosen lixiviant system should be capable of dissolving the metal of interest from the host mineral(s), ideally with preferential dissolution of value minerals over gangue minerals. Environmental impact is an additional important consideration with regards the lixiviant choice. (iii) Access to value minerals; the economic success of an operation depends on the extent of valuable metal recovery within a certain timeframe. ISR has been applied to readily permeable rock because solution flow is possible in these deposit types. Hard-rock environments pose a greater challenge because of the lack of contact of solution with the value mineral, and furthermore, aspects such as vein-hosted or disseminated mineralisation need to be considered. It is also preferable that reaction products do not limit further dissolution, such as by impermeable product layer formation (passivation) or precipitation, which could block solution flow.

This paper presents current options for access creation and permeability enhancement. The most advanced approach includes hydraulic fracturing, while blasting presents an attractive technology for creating fractures in rock. Less traditional access-creation methods and options for enhancing lixiviant/rock contact include waterless fracturing, high-pressure gas generation, cementitious agents, electric discharge, electrokinetics, ultrasonics, microwave fracturing, shape-memory alloys, cryogenic fracturing and the use of surfactants. Permeability enhancement can also be achieved by natural access creation that results from leaching (although flow reduction may occur by chemical precipitation and/or product layer formation).

Definitions and techniques for measuring porosity and permeability are discussed and options for permeability enhancement, their status and various merits, and other influencing factors are provided.

Keywords: In-situ recovery, Access creation, Porosity, Permeability enhancement

INTRODUCTION

Of the deposits processed to date by in-situ recovery (ISR), most have targeted permeable ore (primarily uranium and, more recently, copper). ISR has increased in relevance with considerations of environmental, social, and governance issues and with industry exploring alternative options to conventional processing. Three criteria are critical for the successful implementation of ISR; namely, (i) sufficient contact of the leach solution with the value minerals, (ii) suitable reaction chemistry and value metal dissolution, and (iii) solution containment within a desired region.

Uranium ISR has been practised for over fifty years, but there is recent interest in the application of ISR to deposits other than permeable uranium deposits. One such example includes trials for copper ISR at Excelsior's Gunnison Copper and Taseko's Florence Copper projects in the USA [1,2]. Statistical analysis of drill core of the Florence Copper deposit indicates an average of 11 to 15 open fractures per foot in the fractured oxide zone coupled with oxidised copper mineralisation along these fractures, which provides sufficient flow and leachable mineralisation for ISR without the creation of additional access [3]. In contrast, the sulfide zone beneath the oxidised zone in the Florence Copper deposit contains an average of 6 to 10 closed fractures per foot, and so, is significantly less permeable and amenable to leaching. The application of ISR to hard-rock deposits remains challenging primarily because of the first criterion mentioned above, namely, insufficient solution access to the minerals of interest.

Ideal ranges for deposit permeabilities for ISR are of the order of hundreds of millidarcies [4], but hard-rock samples may have permeabilities in the range of microdarcies. Techniques such as hydraulic fracturing have been applied in the oil and gas industry to increase access and production. Although such techniques are transferrable to the ISR field, more closely spaced access creation may be required for the leaching of disseminated value minerals.

This paper provides background on porosity, permeability, and its measurement; discusses techniques for access creation and overcoming limited permeability; and provides insight into the outlook for hard-rock ISR.

POROSITY AND PERMEABILITY

Definitions

Porosity and permeability are two important parameters related to fluid flow in an in-situ environment.

Porosity

Porosity (ϕ) is defined as the ratio of pore space volume (V_p) to the total volume (V_t) in rock and is expressed as a dimensionless number between 0 and 1 or as a percentage [5,6]:

$$\phi = \frac{V_p}{V_t} \quad (1)$$

Rock porosities vary from rock types with higher porosities, such as sandstones, to rock types with low to zero porosity in igneous rocks. Table 1 provides typical porosities for various rock types [6]. Values in Table 1 serve as a guide, and rock porosities of typical rock types vary based on factors such as fracturing and cementing.

Table 1: Typical porosities for various rock types (from [6])

Rock type	Porosity, ϕ (%)
Narrowly graded silt, sand, gravel	30–50
Widely graded silt, sand, gravel	20–35
Clay, clay-silt	35–60
Sandstone	5–30
Limestone, dolomite	0–40
Shale	0–10
Crystalline rock	0–10
Massive granite	0–0.5

Natural fractures in rock may result in the formation of some degree of overall porosity [5]. Even if fractures comprise only a small component of the total porosity, they may contribute significantly to fluid flow [6]. Intragranular porosity refers to pores within solids and intergranular porosity refers to an interconnected network of pores between solid mineral grains. Intra- and intergranular pores may be catenary (they communicate with others by more than one throat passage), cul-de-sac or dead-end (only one throat passage that connects with another pore), or closed (no communication with other pores) (Figure 1) [7]. Dead-end or

closed pores contribute only marginally or not at all to flow and therefore, the effective porosity (ϕ_e) is defined as the porosity that contributes to flow, with V_p being the volume of voids that is interconnected and transmits flow [6]. The effective porosity decreases compared with the actual porosity as the number of dead-end or closed pores increases.

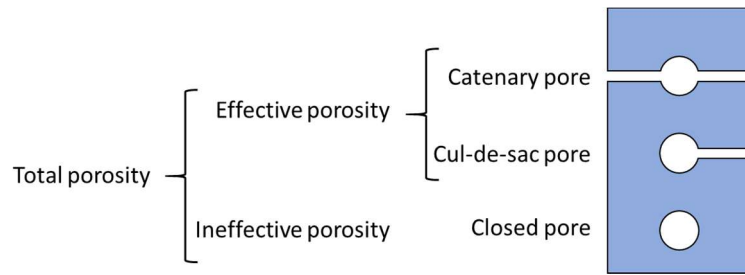


Figure 1: Schematic description of three basic pore types (after [7])

Permeability

According to Darcy's Law, the volumetric flow rate of water Q ($\text{m}^3 \text{s}^{-1}$) that flows between two points is equal to:

$$Q = -\kappa \frac{dh}{dL} A \quad (2)$$

where h is the hydraulic head (m), L is the length (m), A is the cross-sectional area (m^2) and κ is the hydraulic conductivity (m s^{-1}) [5,8]. The negative sign in Eq. (2) indicates that the head decreases in the direction of flow. Darcy's Law is applied in groundwater flow but its application is limited in irregular media or media with large pores and high flow velocities. Typical values of hydraulic conductivity are provided in Figure 2 for various rock types, including that of the oxide and sulfide zones in the Florence Copper deposit [3].

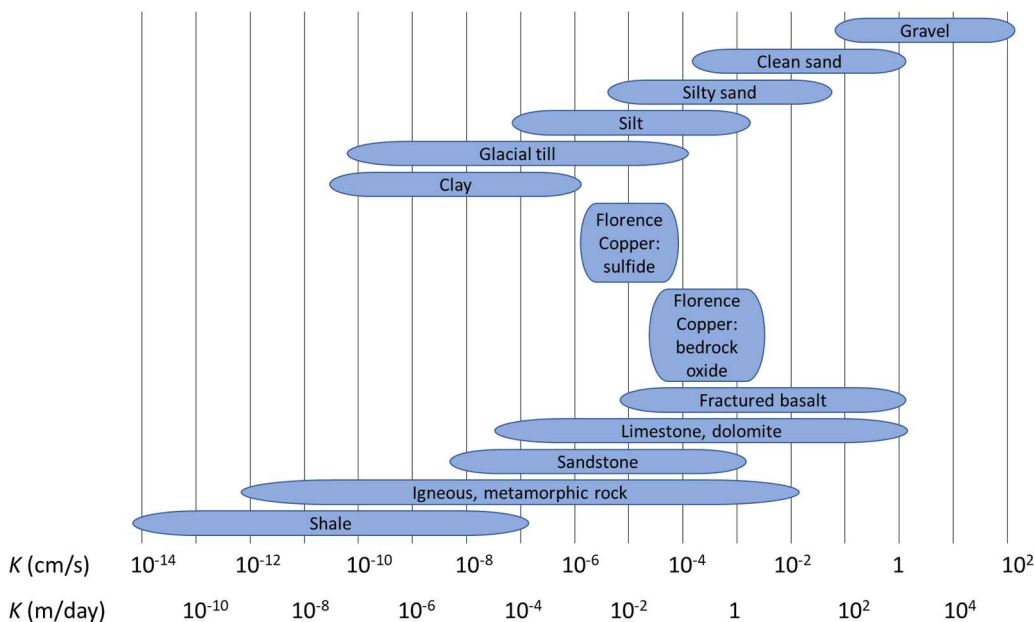


Figure 2: Typical values of hydraulic conductivity, including that of the oxide and sulfide zones in the Florence Copper deposit (after [8])

The hydraulic conductivity parameter is specific to and is a measure of the ease with which a medium transmits water. For the flow of other fluids, the intrinsic permeability is used instead. Intrinsic permeability is independent of fluid properties [8]. The intrinsic permeability describes a rock's ability to transmit fluids, with permeable formations, such as sandstones, having large, interconnected pores that transmit fluids easily, and impermeable formations, such as shales and siltstones, having fine or mixed-size grains with smaller or fewer interconnected pores [5].

The intrinsic permeability k (m^2) is related to the hydraulic conductivity as follows:

$$k = \frac{\kappa_{II}}{\rho g} \quad (3)$$

where μ is the dynamic viscosity (Pa·s), ρ is the density of water (kg m⁻³) and g is the gravitational acceleration (m s⁻²) [8]. The main factor that determines a medium's resistance to flow is the cross-sectional area of its pores, and therefore, it makes sense that k has units of area. The darcy is used as a common unit of intrinsic permeability in petroleum studies, where one darcy is approximately equal to 10⁻⁸ cm² [8].

Water moves with varying velocities and in varying directions through rock. Volume-average descriptors (such as average velocity) rather than small-scale variations are used in the application of Darcy's Law, and irregular, complex reality is represented as a simple, continuous, homogeneous medium [8]. This approach is termed the continuum or macroscopic approach and becomes valid for a large representative block size in a deposit, which is termed the representative elementary volume. The representative elementary volume for fractured rock is larger than for granular media and may be very large or ill-defined if the fractures are widely spaced with irregular apertures [8].

Measurement

Porosity

Porosity may be measured by a variety of laboratory or field-based techniques. Laboratory techniques for cores include mercury porosimetry, nuclear magnetic resonance, and computed tomography. In the field, open-hole geophysical well logs, including neutron, density, and sonic/acoustic logs, and seismic data may correlate with or be used to calculate porosity [5,9,10].

Permeability

The hydraulic conductivity can be estimated in the laboratory or in field experiments [8].

- Correlations of grain size with hydraulic conductivity have been developed, such as by the Hazen or Kozeny–Carman empirical equations.
- Laboratory hydraulic conductivity tests usually make use of intact core and permeameters, in which flow is induced through a saturated sample and Darcy's law is applied to estimate the hydraulic conductivity.
- In the field, slug, pumping, or tracer tests can be used.
 - In a slug test, a sudden well head change is made (for example by insertion or withdrawal of a cylinder) and the time taken for the head to return to equilibrium is recorded to provide an estimate of the average horizontal hydraulic conductivity of a region around the well screen.
 - Pumping tests are used to evaluate larger volumes of material than a slug test (and with a correspondingly increased cost and effort). In pumping tests, changes in the head in the pumping well or nearby observation wells are monitored as a result of a large volume of water being pumped into the well.
 - The hydraulic conductivity may be estimated from the average linear velocity of a tracer (such as heated water or a solute) that is pumped subsurface. Tracer movement may be monitored via wells or by using surface geophysics, such as surface resistivity. Another tracer technique is the borehole dilution test in which the rate of decreasing tracer concentration is measured as a proportional indicator of the fluid discharge from the well.

Flow in fractured rock can be analysed by discrete fracture or by treating the network of fractures as a continuum [8]. The former technique can only be used when the scale of the problem is of the same order of magnitude as the scale of the fracture spacing. In the continuum approach, the rock mass is assumed to be equivalent to a porous medium with homogeneous conductivities. To use such an approach, analysis must be conducted at a scale that is larger than the representative elementary volume (described above).

In massive crystalline rock, porosities are often less than 1% [6]. Figure 3 provides a plot of the permeabilities and porosities for various global copper–gold porphyry ores and shows that the permeabilities of these samples are well below the desired order of hundreds of millidarcies for adequate fluid movement [11].

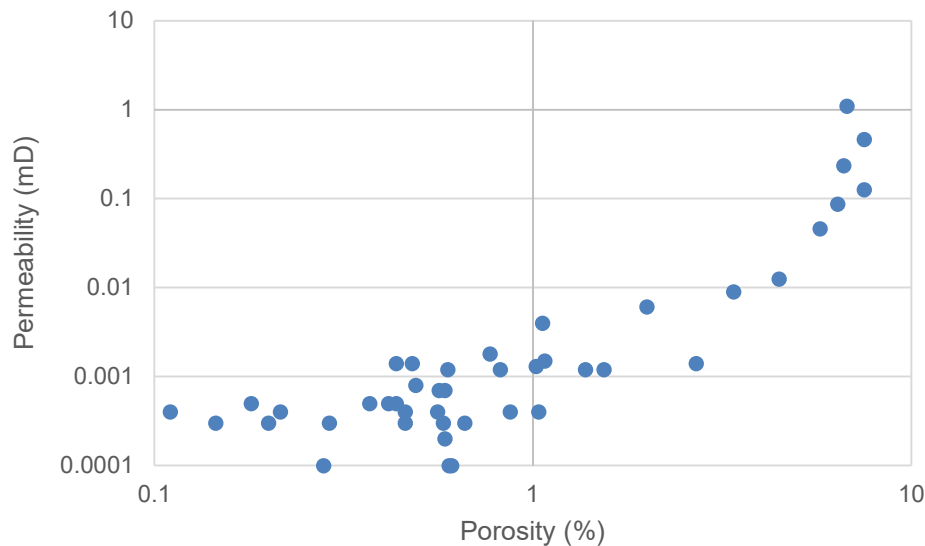


Figure 3: Plot of permeabilities and porosities for various global copper-gold porphyry ores [11]

TECHNIQUES FOR ACCESS CREATION AND OVERCOMING LIMITED PERMEABILITY

The main approach for increasing lixiviant/rock contact is by increasing access into rocks. A common approach to access creation, especially in the oil and gas industry is by hydraulic fracturing. Blasting is another commonly used option for increasing surface area exposure. Other techniques at various stages of research and development include waterless fracturing, high-pressure gas generation, cementitious agents, electric discharge, electrokinetics, ultrasonics and low-frequency vibration, microwave fracturing and shape-memory alloys. Furthermore, lixiviant access is created naturally as value and gangue minerals are leached, and surfactants have also been used to improve fluid contact with ore. An overview of these techniques is provided in subsequent sections.

Hydraulic fracturing

In hydraulic fracturing, high-pressure fluid is injected into a wellbore, and when the fluid pressure exceeds the lithostatic pressure (mass of the rock above where the pressure is applied) and local rock resistance, a fracture is created [12]. Hydraulic fractures tend to propagate perpendicular to the minimum horizontal stress in a plane and may extend for several hundred metres with sufficient pressure exertion [12,13]. Fracturing fluid includes suspended proppants to prop open the network of fractures that develop. Hydraulic fracturing has been used extensively in low-permeability rocks, such as tight sandstone, shale, and some coal beds as a well stimulation technique to increase oil and/or gas flow to wells, and to improve the permeability of geothermal reservoirs.

Hydraulic fluids tend to be water-based and disadvantages of such fluids include water wastage; clay swelling, which blocks channels; groundwater contamination and expensive sewage treatment [13,15,16]. To address these problems, waterless fracturing methods have been developed, as described in the subsequent sections.

Waterless fracturing

Foams, which involve water stabilisation with CO₂ and N₂ have been used to reduce the volume of water required in hydraulic fracturing (and induce more complex fractures), but they tend to be sensitive to high temperatures and salinities and have a higher breakdown pressure than water under the same stress conditions [13,17]. Waterless fracturing, such as the use of oil or gas (gaseous nitrogen (GN₂) and carbon dioxide (CO₂)) with low viscosities and high diffusivities in downhole conditions, may provide an opportunity to overcome these problems. The examples of waterless fracturing technologies below have been tested at the laboratory and field-scale in oil and gas production.

Oil-based fracturing

Oil-based fluids (such as gasoline, kerosene, diesel and crude oil) may be used preferentially in cold regions where the freezing of water may be problematic [13]. However, such fluids can reduce permeability and may be expensive and difficult to dispose of. CO₂ or N₂ may be added to the fracturing fluid to reduce the volume of oil required and aid with flow, and such fluids are termed “energized”.

Gelled alcohol and liquified petroleum gas fracturing

Alcohol and liquified petroleum gas have shown potential for use as non-aqueous fluids in fracturing [13]. Crosslinked gels, such as gelled methanol, have been used to increase the fluid viscosity, which facilitates proppant transport.

Gas/pneumatic fracturing

Gas or pneumatic fracturing, for example, with nitrogen or carbon dioxide generally allows for a reduced breakdown pressure and more complex fracture morphology than water fracturing [18]. Gaseous nitrogen provides an affordable option as an inert material for injection at pressures that are high enough to fracture rock, however, the low density and viscosity of nitrogen limit proppant transport [13]. Non-cryogenic CO₂ can also be used in fracturing, with the CO₂ evaporating after treatment and returning to the surface at a controlled rate as a gas [13].

Cryogenic fracturing

In liquid nitrogen (LN₂) fracturing, the temperature change from rock/LN₂ contact results in a sharp reduction in temperature, mineral grain shrinkage and deformation, and an increase in fracture density (primary and secondary cracks that are perpendicular to the primary fractures) [14,16]. Thermal stress is generated by the temperature gradient and the mismatched deformation of adjacent minerals, and fracturing results when this thermal stress exceeds the cementing stress [14]. If liquid is present in the pores, LN₂ contact freezes the fluid, which expands and damages the pore structure by exerting compressive stresses [16]. Different rock types with different water contents respond differently to LN₂, with results including a decrease in the number of pores and their volume, an expansion of microfissures (micropores), an increase in pore scale, and the generation of macrocracks. For example, Cai et al. [16] found that the number and volume of pores in a dry sandstone (with large, loosely arranged mineral grains and existing fractures) decreased after LN₂ contact, whereas the microfissures expanded and the pore volume increased in dry marble and shale because these rock types had few initial fractures and small and compactly arranged initial mineral grains that shrank when exposed to LN₂ [16]. Saturated samples showed an intensified damage with LN₂ exposure. Initial field applications have indicated the viability of the technology, but further work is required to ensure wide uptake [14].

In cryogenic CO₂ fracturing, pre-cooled proppants are mixed with 100% liquid CO₂ and pumped into wells [15]. Advantages of the use of cryogenic CO₂ include its low surface tension and ability to flow, which provide it with a strong mobility and therefore, rock-breaking capacity. Problems related to this technology include the high friction of liquid CO₂; its low viscosity, which makes proppant carrying difficult and results in large amounts of fluid loss; challenging phase control; immature fracturing equipment and underdeveloped computational methods for operating parameters [15].

Supercritical fluid fracturing

Supercritical CO₂ has also been investigated for use in rock breaking [19,20,21]. Supercritical CO₂ is a non-gaseous, non-liquid, non-solid CO₂ that exists above temperatures of 304 K and pressures above 7.38 MPa, and has a higher diffusivity, lower viscosity and lower surface tension than liquid CO₂ (Figure 4) [19].

Hydrothermal spallation is a drilling technique that makes use of supercritical water (pressure > 22.4 MPa, T > 647.1 K/374°C), oxygen and fuel (such as methanol) to drill in hard and brittle rock, such as granite [22]. A high-temperature medium is generated by the reaction between the fuel and oxygen at the rock surface, which results in the induction of a non-uniform thermal stress because of the difference in temperature in the rock interior.

Supercritical CO₂ has a higher temperature than LN₂, and therefore, may induce weaker thermal shock in rock formations [14].

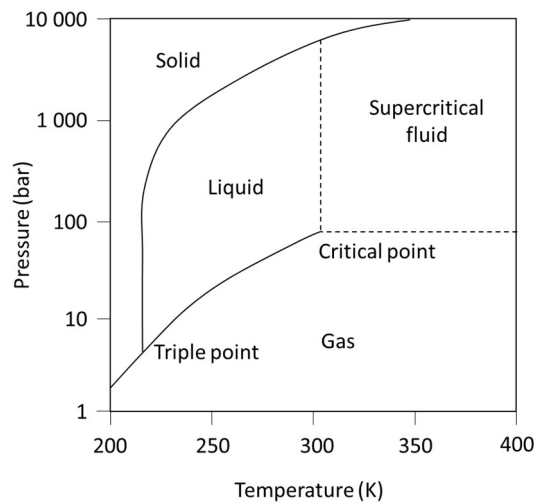


Figure 4: Carbon dioxide pressure-temperature phase diagram

Blasting

Mechanical energy, such as is used in comminution, may be 50 times less efficient than chemical energy that is used, for example, in the form of commercial explosives in blasting, and therefore, blasting serves as a potential attractive option for access creation [23]. Furthermore, like hydraulic fracturing, blasting is a mainstream technology in the mining industry. Blasting may be used to complement hydraulic fracturing. The fracture mechanism in blasting involves the creation of branching from multiple nucleation points and the development of a branched fracture network. Fractures from blasting occur primarily parallel to the maximum principal stress, as opposed to hydraulic fracturing that produces single continuous fractures perpendicular to the borehole [23].

The blasting rate of reaction (microseconds) is faster than that of hydraulic fracturing, with advantages and disadvantages from this rate. Blasting can be applied in a confined (infinite rock mass) or unconfined environment (finite rock mass). In the former, all surfaces may transmit explosive-induced stress waves, without reflections from any surface, and damage is constrained around the blasthole. In the latter case, stress waves may be reflected rapidly from the unconfined surface (or from layers of different rock types), which results in greater damage and fracturing and fragmentation over a larger area than in the confined case [23].

The advantage of the increase in damage in unconfined rock has led to the proposal for hybrid mining systems that allow for a small amount of relief by the removal of a portion of material. For example, Orica has conducted studies with hydraulic fracturing as a pre-conditioning tool prior to blasting and found that hydraulic fracturing with proppant allows for increased damage, a reduced stress state in the damage envelope, and can increase the permeability [23]. Dare-Bryan and Boyce [23] have described the use of the remote ore extraction system (ROES) to create underground in-mine leach reactors in which horizontal rings of holes are drilled from a central raise-bored hole. The rings are blasted downwards, and a small amount of material is extracted from the lower development level to provide relief and produce a silo of fragmented rock, which simulates an underground in-situ heap leach. Lixiviant percolates through the ore and is collected for pumping to the surface.

High-pressure gas generation

Cardox, Nonex and penetrating cone fracture (PCF) are popular high-pressure gas generators with an increasingly widespread use in rock-breaking [24]. Fracturing is achieved by ignition of a propellant inside a tube, which releases high-pressure gas, such as carbon dioxide, water, nitrogen, carbon monoxide and hydrogen, through fissures and microcracks in rock, and results in breakage in tension (rather than in compression, as is achieved with explosives). The high-pressure gas generation yields less energy dissipation on breakage and is used particularly when noise, vibration, and dust release need to be minimised.

Cementitious agents

Cementitious powdery substances that are a combination of Portland cement clinker that is mixed with gypsum, blast furnace slag, polyhydrate, limehydrate and aluminium hydroxydochloride have been used as expanding powders to break rock [25,26]. When mixed with water in a confined space, the powders hydrate (to form, for example, ettringite and calcium oxide) and expand 20% to 30% within 6 to 24 h with an increase in temperature of up to 150°C. Cracks form when the expansive pressure exceeds the tensile strength of the rock [26]. Commercial expanding powders include Betonamit, Bristar, Cevamit, Dexpan, Ecobust, Expando, S-Mite, and Acconex. Compared with hydraulic fracturing, fracturing with cementitious agents could reduce the quantities of water required, downhole tools, number of fracturing pump trucks, and the total operational

cost [26]. Cementitious agents may be less suitable in saturated environments, where they can be washed out, and their viscosity increases after mixing, so they may not be able to maintain workability for a prolonged period. De Silva et al. [27] studied lime hydration and the formation of $\text{Ca}(\text{OH})_2$ from CaO as a technique for fracture stimulation and found, by three-dimensional modelling, that a tenfold increase in fracture density and denser and controllable fracture network could be achieved compared with conventional hydraulic fracturing.

Electric discharge

Two forms of electric discharge include (i) the placement of electrodes directly on rock, with the generation of a high-pressure short pulse, a plasma discharge inside the rock, and breakage from expansion of the plasma channel inside the rock with mineral components of different permittivities and electrical conductivities (termed electrical/electro-pulse fragmentation) or (ii) generation of an electric arc in a liquid, which induces a mechanical force (such as a compression shock wave, bubble collapse or pressure wave) that is transmitted to the rock (electrohydraulic fragmentation) [12,28,29,30].

Electrical and electrohydraulic fragmentation were first studied in the 1950s and 1960s, respectively. Electrohydraulic fragmentation is achieved by compressional forces from shock waves, whereas electric fragmentation induces tensional forces from the expanding plasma channel [31]. Rock tensional strength is 4%–15% of its compressional strength, and therefore, the electrical fragmentation technique generates better breakage for the same amount of power [31]. Electrical fragmentation also allows for a more rapid propagation of electric pulses than in water [28] and is a form of dynamic loading in which a large amount of energy is forced into a small volume of material and yields distributed microcracking [12]. Such damage contrasts with static loading, in which the surface of a crack is proportional to the energy that is transferred to the volume of material that breaks and localized, large cracks result (such as in hydraulic fracturing).

In electrohydraulic laboratory experiments with electrodes in a borehole filled with water, Chen et al. [29] found that an increase in electrical energy and number of shock waves increased the permeability of cylindrical mortar and sandstone samples by at least two orders of magnitude. A threshold energy needs to be exceeded before damage and an increased permeability result, and this threshold increases with an increase in specimen confinement stress. The extent of damage is estimated to be in the 2 to 4 m range [12] and the combined use of electrohydraulic and hydraulic fracturing has been proposed.

In electrical breakage, high voltages are required to reach the electric breakdown strength of rock (e.g., 100–150 kV/cm for granite) [32] and the voltages must be increased sufficiently rapidly to allow for breakdown (plasma) channel creation in the rock rather than in the liquid. Energies, plasma channel widths, temperatures and pressures may reach 100 J/cm, 10–50 μm , 10^4 K and 10^9 Pa, respectively. The method has been applied in comminution applications, such as in the SELFRAG instrument [33]. In laboratory tests, Van der Wielen et al. [34] varied the SELFRAG voltage, electrode gap, pulse rate and number of electrical pulses and found that the total applied energy (which is controlled by the number of discharges and voltage) is the main variable that affects product size, an increase in pulse rate improves the probability of discharge, and coarse particles were more amenable to breakage than fine particles. The acoustic impedance, porosity and quartz content were also correlated with breakage behaviour. Zuo et al. [35] investigated the effect of specific energy, pulse voltage, cumulative discharges, feed particle size and ore particle breakage pattern (body breakage or surface breakage) on the particle breakage behaviour of (i) a copper–gold ore with finely disseminated metalliferous minerals in veins, (ii) an iron oxide copper–gold (IOCG) ore and (iii) a highly porous hematite ore. They found that the mass-specific energy was the most significant factor that affected the breakage behaviour.

Electrokinetics

Electrokinetics has been proposed as an option for application in deposits of limited permeability [36,37]. Electrokinetics involves the application of an electric field to induce a controlled migration of lixiviant through rock. Electrokinetics has been used in soil remediation and for metal recovery from fly ash, wastewater sludge and tailings [37,38], and research into its novel application for ISR is being conducted [36,37]. Martens et al. [36,37] confirmed the in-principle feasibility of the use of electrokinetics to leach gold from an unconsolidated porous media using an iodide/tri-iodide solution and copper from chalcopyrite, covellite and chalcocite in a sulfidic porphyry ore sample (6.1 mD permeability, 11% porosity) using a ferric/hydrochloric acid solution. Karami et al. [39] used a standardised laboratory setup to confirm that an increase in applied voltage increased ion migration and that a reduced synthetic core permeability hindered lixiviant ion migration. Martens et al. [37] modelled, using a reactive transport simulation, the copper extraction from a theoretical copper deposit (0.4 wt% Cu) and found a ~70 wt% recovery within three years with 5-m-spaced electrodes.

Ultrasonics and low-frequency vibration

Earthquakes and seismic activity have resulted in increased oil production from oilfields, which led to the principle of seismic stimulation to improve oil recovery [40]. Seismic stimulation has been applied by (i) pulsed fluid injection from the borehole to generate seismic waves, (ii) usage of a surface-based vibrator (usually a

large weight that impacts the ground periodically), (iii) use of a sonic or ultrasonic generator to transmit vibro-energy or (iv) chemical or nuclear reaction explosion downhole or at the surface [40]. High-frequency waves (e.g., 20 kHz) are usually applied in near-wellbore stimulation and low-frequency waves (e.g., 40 Hz) cover a large region and are used for reservoir-scale simulation.

Ultrasonic and low-frequency vibrations have been tested to improve the leaching efficiency in low-permeability sandstones [41]. Zhao et al. [41] found that the uranium leaching performance and permeability of low-permeability sandstone cores (0.05–1.98 mD) improved by up to six times with low-frequency vibration (0.01 Hz to 100 Hz) and was approximately nine times more effective than ultrasound (>20 kHz). Low-frequency vibration improves fluid permeability by physical vibration and ultrasonics produce cavitation by a sonochemical reaction. Besides improving the permeability, the vibration can improve the leaching and reaction rate.

Tests at the Dolmatovo uranium deposit, Russia, were undertaken using a vibration exciter (manufactured by the Institute of Mining, Siberian Branch of the Russian Academy of Sciences) to establish whether low-frequency seismic excitation (~8.5–11.5 Hz, seismic capacity of 30–40 kW, seismic field intensity of $0.8\text{--}1 \times 10^{-3} \text{ W/m}^2$, 0.2–0.4 μm particle vibro-displacements) could influence the filtration and production capacities from the uranium-bearing rock formation [42]. Flaky clay in the Dolmatovo deposit is associated with tightly bound water, which prevents capillary substitution by leaching solutions. As a result, the deposit has a 1–2 m/day filtration factor and a water transmissibility of 10–15 m^2/day , compared with commercial deposits in Kazakhstan of 10–20 m/day. The deposit transmissibility increased by 10% and the solution metal contents increased by 10%–20% within a week after treatment.

Microwave fracturing

Research into the microwave heating of ore was initiated in 1966 [43]. Microwave energy is a form of electromagnetic energy that travels as high-frequency waves with wavelengths between 1 mm and 1 m and frequencies between 0.3 and 300 GHz [43]. When applied to a material, rapid changes in electric and magnetic components in the material lead to friction and the conversion of electromagnetic to heat energy. Microwave heating is influenced by water content, power level, microwave frequency, and material characteristics [44].

Microwaves obey the laws of optics and can be transmitted, absorbed, and reflected [45]. Three main groups of materials include (i) transparent or low-loss materials through which microwaves pass without loss (microwave-transparent), such as aluminosilicates, micas, carbonates and sulphates), (ii) conductors that reflect microwaves, without penetration and (iii) absorbing or high-loss materials that absorb microwaves and dissipate electromagnetic energy as heat (microwave-absorbent) depending on their dielectric loss factor (the ability of the material to dissipate the stored energy as heat), such as sulfides and metal oxides [43,44,46]. When two or more phases with different dielectric properties exist, selective heating can be obtained in high-loss phases. Materials with more than one phase with different heating rates allow for the expansion of different minerals and thermally induced crack generation along grain boundaries (most likely between absorbent and transparent species), liberation, an increase in surface area and a reduction in ore competency [43,44,47,48]. Temperatures of up to 1000, 980, 700, 700, 650, 510, 400, 380 and 160°C for titanomagnetite, hematite, bornite, magnetite, galena, molybdenite, chalcopyrite, pyrrhotite and sphalerite were achieved with microwave heating at 500 W and 2450 MHz for 4 min [49].

Microwave treatments of up to 25 kW with energy inputs of 0.5–10 kWh/t showed that greatest reductions in strength resulted for materials that contained 2 wt% to 20 wt% microwave-absorbing minerals with a grain size greater than 500 μm and constrained by hard matrix minerals, such as quartz and feldspar [47]. Microwave treatment has progressed to pilot-scale (150 tph) and, although no sub-surface implementation has been attempted for ISR, Li et al. [50] and Ovalles et al. [51] describes the potential for microwave application in coalbed methane and oil extraction by using wave guides and antennas to achieve microwave irradiation down boreholes [52].

Shape-memory alloys

Shape-memory alloys (SMAs) can revert from a deformation and generate high stresses in response to thermal or mechanical stimuli [53]. If the deformed material aims to recover its shape (such as expand to its original shape) and is placed in a constrained environment, large forces may be generated with the application of heat. High-force, high-temperature SMAs have been developed for space-related applications (such as on the moon, Mars and near-Earth asteroids), where controlled, compact, reliable and cost-effective geologic excavation is required [53]. Various SMAs have been developed, including Fe-, Co(+Ni,Se,Ge,Al)- Cu-, Zr-, FeMnSi(+Co,Ni,Cr)-, CuAlNi(+Mn,Ti,B,Zn)-, CuAlAg-, CuAlNb-, NiMn(+Al,Ti,Cu,Co,Cr)-, NiAl(+Fe,B,Cu,Co,Ag,Re)-, TiPt(Pd,Au,Rh)-, NiTiCu-, NiTiHf-, NiTiZr-, NiTi-, NiMnGa-, NiTiPd-, TaRu-, NbRu-based based alloys [53,54]. Examples of alloys, applied temperatures and their corresponding recovery forces include: NiTi/90–95°C/566–800 MPa, NiTiCu/66°C/650 MPa, NiTiHf/> 100°C/> 1.5 GPa.

Surfactant use

Surfactant addition has been shown to enhance fluid contact with ore by a decrease in liquid surface tension or viscosity, which allows for (i) a better wetting behaviour and stronger spreading ability, (ii) a reduced liquid film thickness and increased mass transfer rate and (iii) greater adsorption into fissures in the ore surface [55,57]. Anionic, cationic and nonionic surfactants may allow for a change in electrical properties of the ore surface, which may also enhance leaching [55]. Surfactants that have been investigated in experimental studies include sodium dodecyl sulfate, dodecyl trimethyl ammonium chloride/bromide, tetradecyl trimethyl ammonium chloride, cetyltrimethyl ammonium chloride/bromide, stearyltrimethyl ammonium chloride, dodecyl dimethyl benzyl ammonium chloride, polyoxyethylene octylphenol ether and polyoxyethylene octyl phenyl ether [16,55,56]. For example, in column leaching experiments to simulate heap leaching of a copper ore, Ai et al. [55] found that sodium dodecyl sulfate reduced the surface tension of a 20 g/L sulfuric acid lixiviant by more than 50%, doubled the permeability coefficient relative to the control and increased the copper extraction by 8%. In a study on the in-situ leaching of low permeability sandstone ores, Tan et al. [57] found that uranium leaching from columns using 10 g/L sulfuric acid and polyoxyethylene octyl phenyl ether and perfluoroalkyl sulfuryl fluoride surfactants (10 mg/L) resulted in an increased permeability coefficient of 42%–87% and an increase in uranium extraction by 58%. Du et al. [58] found that the surface tension decreased by up to 13% and the uranium extraction increased by up to 19% when 1 mg/L anionic surfactant polyoxyethylene ether heptamethyltrisiloxane was used in a $\text{Na}_2\text{CO}_3/\text{NaHCO}_3$ leach.

Chemical dissolution

During leaching, the ore porosity and permeability change because of mineral dissolution and/or precipitation. Zeng et al. [59] used nuclear magnetic resonance to study the effect on permeability of the acid leaching of uranium-hosted sandstone and found that the permeability increased because of mineral dissolution. However, physical sedimentation (fine particle migration and blockage of permeable passages) and chemical sedimentation (from precipitation of poorly soluble substances such as CaSO_4 and MgSO_4) decrease permeability [55], and Zeng et al. [59] also found that the permeability of samples in their studies decreased with precipitate formation. Gypsum formed at a lower pH and with an increased acid consumption and subsequent increase in pH, iron (pH 2.5–3.5) and aluminium (pH 3–4) hydroxide precipitates formed, which reduced the pore connectivity and seepage rate. Flow through the media resulted in the blockage of pores by small particles (such as from clay minerals).

Gypsum and jarosite precipitation was found to reduce the flow rate at the Cyprus Casa Grande ISR operation (Colorado, USA) [60]. Precipitate formed in 10%–90% of the deposit with a decrease of 0.2 mD to 0.11 mD per 100 mL injected lixiviant and 25 cm³ total precipitate formed per gram of copper recovered.

In anoxic acid leaching of coarse-grained bornite/chalcocite samples, Hidalgo et al. [61] describe that mineral phase transformations and replacements resulted in an increased porosity. In high-temperature chalcopyrite leaching in acidified solution with oxidant, chalcopyrite cuboids of ~4 mm × 4 mm × 4 mm underwent a volume reduction of 10.3% with a 95.6% increase in surface area and an increased porosity [62]. The copper-containing cubes showed a replacement of the initial solid by copper-enriched secondary sulfides and sulfur as a final product along access zones, and the number of fractures and their size increased after the reaction. It was also found that akaganeite precipitated in chloride systems and jarosite and gypsum formed in sulfate systems in the second stage of a five-stage acidified re-contact leach of copper sulfide ores with oxidant [63]. In this same study, which aimed to simulate what may occur in an ISR environment, 'rugosity' was used as an indicator of the development of particle porosity. Rugosity is the ratio between the intrinsic area (including the cracks and/or pores) and the characteristic area (the spherical particle surface that is projected as a plane), with a higher ratio indicating a higher porosity of presence of surface irregularities [63]. The rugosity increased after the five leaching stages. In a study of the sulfuric-acid leaching of individual particles from a vanadium-titanium deposit, leaching was found to occur by a shrinking-core mechanism or by access via cracks or grain boundaries [64].

CONCLUSIONS AND OUTLOOK FOR ISR

The deposit porosity and permeability may provide an indication of the potential for fluid movement in ISR operations, but it is the latter property that is most important in terms of lixiviant access and contact with leachable mineralisation. Slug tests, pumping tests and tracer tests may be used in the field to estimate the potential for fluid flow. Deposits with low permeabilities (below the order of hundreds of millidarcies) may require the creation of additional access for lixiviant/rock contact.

Hydraulic fracturing and blasting are the most developed access-creation technologies for immediate application to ISR. Besides these two techniques, several additional access-creation techniques, including waterless fracturing, high-pressure gas generation, cementitious agents, electric discharge, electrokinetics,

ultrasonics, microwave fracturing, and shape-memory alloys have been investigated at the laboratory scale. However, these techniques are not sufficiently mature for application in the field, and they require additional research and scale-up to field trials. Chemical dissolution and the use of surfactants provide an additional means for permeability creation and enhanced mass transfer or solution contact with mineral surfaces, respectively.

The further progressing and development of the technologies described in this paper has the potential for solving one of the greatest challenges in ISR, namely access to value minerals, and unlocking the option for hard-rock processing.

REFERENCES

1. Website: <https://www.excelsiormining.com/projects/gunnison-copper-project>, accessed 22 March 2022.
2. Website: <https://www.tasekomines.com/properties/florence-copper>, accessed 22 March 2022.
3. Johnson D (2017) NI 43-101 Technical Report, Florence Copper Project, Florence, Pinal County, Arizona, Taseko Mines Limited.
4. Sinclair L, Thompson J (2015) In situ leaching of copper: Challenges and future prospects, *Hydrometallurgy*, 157, 306–324.
5. Guo B (2019) Petroleum reservoir properties, Editor: Guo B, *Well Productivity Handbook (Second Edition)*, Gulf Professional Publishing, pp. 17–51.
6. Fitts CR (2013) Physical Properties, Editor: Fitts CR, *Groundwater Science (Second Edition)*, Academic Press, pp. 23–45.
7. Selley RC, Sonnenberg SA (2015) The Reservoir, Editor(s): Selley RC, Sonnenberg SA, *Elements of Petroleum Geology (Third Edition)*, Academic Press, pp. 255–320.
8. Fitts CR (2013) Principles of Flow, Editor(s): Fitts CR, *Groundwater Science (Second Edition)*, Academic Press, pp. 47–96.
9. Selley RC, Sonnenberg SA (2015) Methods of Exploration, Editor(s): Selley RC, Sonnenberg SA, *Elements of Petroleum Geology (Third Edition)*, Academic Press, pp. 41–152.
10. Wang F, Cai J (2019) Characterization of Petrophysical Properties in Tight Sandstone Reservoirs, Editor(s): Cai J, Hu X, *Petrophysical Characterization and Fluids Transport in Unconventional Reservoirs*, Elsevier, pp. 37–59.
11. Esteban L (2017) Personal communication, porosity-permeability database, CSIRO Energy.
12. Pijaudier-Cabot G, La Borderie C, Reess T, Chen W, Maurel O, Rey-Berbeder F, de Ferron A (2016) Preface and Introduction, Editor: Pijaudier-Cabot G, *Electrohydraulic Fracturing of Rocks*, pp. xi – xix.
13. Wang L, Yao B, Cha M, Alqahtani NB, Patterson TW, Kneafsey TJ, Miskimins JL, Yin X, Wu Y (2016) Waterless fracturing technologies for unconventional reservoirs-opportunities for liquid nitrogen, *Journal of Natural Gas Science and Engineering*, 35(A), 160–174.
14. Huang Z, Zhang S, Yang R, Wu X, Li R, Zhang H, Hung P (2020) A review of liquid nitrogen fracturing technology, *Fuel*, 266, 117040.
15. Liu H, Wang F, Zhang J, Meng S, Duan Y (2014) Fracturing with carbon dioxide: Application status and development trend, *Petroleum Exploration and Development*, 41(4), 513–519.
16. Cai C, Li G, Huang Z, Shen Z, Tian S, Wei J (2014) Experimental study of the effect of liquid nitrogen cooling on rock pore structure, *Journal of Natural Gas Science and Engineering*, 21, 507–517.
17. Wanniarachchi WAM, Ranjith PG, Perera MSA, Rathnaweera TD, Zhang DC, Zhang C (2018) Investigation of effects of fracturing fluid on hydraulic fracturing and fracture permeability of reservoir rocks: An experimental study using water and foam fracturing, *Engineering Fracture Mechanics*, 194, 117–135.
18. Hou P, Gao F, Ju Y, Yang Y, Gao Y, Liu J (2017) Effect of water and nitrogen fracturing fluids on initiation and extension of fracture in hydraulic fracturing of porous rock, *Journal of Natural Gas Science and Engineering*, 45, 38–52.
19. Wang H, Li G, Shen Z, Tian S, Sun B, He Z, Lu P (2015) Experiment on rock breaking with supercritical carbon dioxide jet, *Journal of Petroleum Science and Engineering*, 127, 305–310.
20. Guo T, Zhang Y, Shen L, Liu X, Duan W, Liao H, Chen M, Liu X (2022) Numerical study on the law of fracture propagation in supercritical carbon dioxide fracturing, *Journal of Petroleum Science and Engineering*, 208(A), 109369.
21. Zhang X, Lu Y, Tang J, Zhou Z, Liao Y (2017) Experimental study on fracture initiation and propagation in shale using supercritical carbon dioxide fracturing, *Fuel*, 190, 370–378.
22. Hu X, Song X, Liu Y, Cheng Z, Ji J, Shen Z (2019) Experiment investigation of granite damage under the high-temperature and high-pressure supercritical water condition, *Journal of Petroleum Science and Engineering*, 180, 289–297.
23. Dare-Bryan P, Boyce P (2019) Potential Use of Blasting to Enhance Permeability, *Proceedings of the ALTA ISR Conference 2019, Perth, Western Australia*.
24. Caldwell T (2005) A Comparison of Non-Explosive Rock Breaking Techniques, *Australian Tunnelling Society Conference*.

25. Res J, Wladzielczyk K, Ghose AK (2003) *Environment-Friendly Techniques of Rock Breaking* (First Edition) Routledge, pp. 15–26.
26. De Silva RV, Pathegama Gamage R, Perera MSA (2016) An Alternative to Conventional Rock Fragmentation Methods Using SCDA: A Review, *Energies*, 9(11), 958.
27. De Silva RV, Pathegama Gamage R, Perera MSA, Wu B, Wanniarachchi WAM (2018) A low energy rock fragmentation technique for in-situ leaching, *Journal of Cleaner Production*, 204, 586–606.
28. Li C, Duan L, Tan S, Chikhotkin V (2018) Influences on High-Voltage Electro Pulse Boring in Granite, *Energies*, 11(9), 2461.
29. Chen W, Maurel O, Reess T, Silvestre De Ferron A, La Borderie C, Pijaudier-Cabot G, Rey-Bethbeder F, Jacques A (2012) Experimental study on an alternative oil stimulation technique for tight gas reservoirs based on dynamic shock waves generated by Pulsed Arc Electrohydraulic Discharges, *Journal of Petroleum Science and Engineering*, 88–89, 67–74.
30. Andres U, Jirestig J, Timoshkin I (1999) liberation of minerals by high-voltage electrical pulses, *Powder Technology*, 104 (1), 37–49.
31. Sperner B, Jonckheere R, Pfänder JA (2014) Testing the influence of high-voltage mineral liberation on grain size, shape and yield, and on fission track and ⁴⁰Ar/³⁹Ar dating, *Chemical Geology*, 371, 83–95.
32. Saksala T (2021) Cracking of granitic rock by high frequency-high voltage-alternating current actuation of piezoelectric properties of quartz mineral: 3D numerical study, *International Journal of Rock Mechanics and Mining Sciences*, 147, 104891.
33. Website: <https://www.selfrag.com>, accessed 22 March 2022.
34. van der Wielen KP, Pascoe R, Weh A, Wall F, Rollinson G (2013) The influence of equipment settings and rock properties on high voltage breakage, *Minerals Engineering*, 46–47, 100–111.
35. Zuo W, Shi F, van der Wielen KP, Weh A (2015) Ore particle breakage behaviour in a pilot scale high voltage pulse machine, *Minerals Engineering*, 84, 64–73.
36. Martens E, Prommer H, Dai X, Wu MZ, Sun J, Breuer P, Fourie A (2018) Feasibility of electrokinetic in situ leaching of gold, *Hydrometallurgy*, 175, 70–78.
37. Martens E, Prommer H, Sprocati R, Sun J, Dai X, Crane R, Jamieson J, Ortega Tong P, Rolle M, Fourie A (2021) Toward a more sustainable mining future with electrokinetic in situ leaching, *Science Advances*, 7(18), 1–10.
38. Karami E, Kuhar L, Bona A, Nikoloski AN (2021) A review of electrokinetic, ultrasonic and solution pulsing methods for mass transfer enhancement in in-situ processing, *Minerals Engineering*, 170, 107029.
39. Karami E, Kuhar L, Bona A, Nikoloski AN (2022) Investigation of the effect of different parameters on lixiviant ion migration in a laboratory scale study of electrokinetic in-situ recovery, *Mineral Processing and Extractive Metallurgy Review*, doi.org/10.1080/08827508.2021.2017924.
40. Sun Q, Retnanto A, Amani M (2020) Seismic vibration for improved oil recovery: A comprehensive review of literature, *International Journal of Hydrogen Energy*, 45(29), 14756–14778.
41. Zhao Y, Gao Y, Luo C, Liu J (2021) Improved uranium leaching efficiency from low-permeability sandstone using low-frequency vibration in the CO₂+O₂ leaching process, *Journal of Rock Mechanics and Geotechnical Engineering*, doi.org/10.1016/j.jrmge.2021.10.013.
42. Makaryuk NV (2009) Seismic vibration treatment of a pay zone for improvement of the filtration and production parameters of underground metal leaching, *Journal of Mining Science*, 45(6), 590–601.
43. Al-Harashsheh M (2004) Microwave-assisted leaching—a review, *Hydrometallurgy*, 73, 189–203.
44. Wei W, Shao Z, Zhang Y, Qiao R, Gao J (2019) Fundamentals and applications of microwave energy in rock and concrete processing – A review, *Applied Thermal Engineering*, 157, 113751.
45. Pickle CA (2009) Microwaves in extractive metallurgy: Part 1 – Review of fundamentals, *Minerals Engineering*, 22(13), 1102–1111.
46. Kingman SW, Vorster W, Rowson NA (2000) The influence of mineralogy on microwave assisted grinding, *Minerals Engineering*, 13(3), 313–327.
47. Batchelor AR, Jones DA, Plint S, Kingman SW (2015) Deriving the ideal ore texture for microwave treatment of metalliferous ores, *Minerals Engineering*, 84, 116–129.
48. Jones DA, Kingman SW, Whittles DN, Lowndes IS (2007) The influence of microwave energy delivery method on strength reduction in ore samples, *Chemical Engineering and Processing: Process Intensification*, 46(4), 291–299.
49. Haque KE (1999) Microwave energy for mineral treatment processes—a brief review, *International Journal of Mineral Processing*, 57(1), 1–24.
50. Li H, Lin B, Yang W, Zheng C, Hong Y, Gao Y, Liu T, Wu S (2016) Experimental study on the petrophysical variation of different rank coals with microwave treatment, *International Journal of Coal Geology*, 154–155, 82–91.
51. Ovalles C, Fonseca A, Lara A, Alvarado V, Urrecheaga K, Ranson A, Mendoza H (2002) Opportunities of Downhole Dielectric Heating in Venezuela: Three Case Studies Involving Medium, Heavy and Extra-Heavy Crude Oil Reservoirs, SPE International Thermal Operations and Heavy Oil Symposium and International Horizontal Well Technology Conference, Calgary, Alberta, Canada, November 2002.
52. Buttress AJ, Katrib J, Jones DA, Batchelor AR, Craig DA, Royal TA, Dodds C, Kingman SW (2017) Towards large scale microwave treatment of ores: Part 1 – Basis of design, construction and commissioning, *Minerals Engineering*, 109, 169–183.

53. Benafan O, Noebe RD, Halsmer TJ (2016) Static rock splitters based on high temperature shape memory alloys for planetary explorations, *Acta Astronautica*, 118, 137–157.
54. Firstov GS, Van Humbeeck J, Koval YN (2006) High Temperature Shape Memory Alloys Problems and Prospects, *Journal of Intelligent Material Systems and Structures*, 17(12), 1041–1047.
55. Ai C, Sun P, Wu A, Chen X, Liu C (2019) Accelerating leaching of copper ore with surfactant and the analysis of reaction kinetics, *International Journal of Minerals, Metallurgy, and Materials*, 26, 274–281.
56. Zhang P, Sun L, Wang H, Cui J, Hao J (2019) Surfactant-assistant atmospheric acid leaching of laterite ore for the improvement of leaching efficiency of nickel and cobalt, *Journal of Cleaner Production*, 228, 1–7.
57. Tan K, Li C, Liu J, Qu H, Xia L, Hu Y, Li Y (2014) A novel method using a complex surfactant for in-situ leaching of low permeable sandstone uranium deposits, *Hydrometallurgy*, 150, 99–106.
58. Du R, Zhang X, Li M, Wu X, Liu Y, Jiang T, Chen C, Peng Y (2019) Leaching of low permeable sandstone uranium ore using auxiliary materials: anionic surfactants, *Journal of Radioanalytical and Nuclear Chemistry*, 322, 839–846.
59. Zeng S, Shen Y, Sun B, Zhang N, Zhang S, Feng S (2021) Pore structure evolution characteristics of sandstone uranium ore during acid leaching, *Nuclear Engineering and Technology*, 53(12), 4033–4041.
60. Earley D, Jones P (1992) *Geochemical effects on the hydrology of in-situ leaching mining of copper oxide ore at the Cyprus Casa Grande Mine, Arizona*. Littleton, CO, United States: Society for Mining, Metallurgy, and Exploration, Littleton, CO, pp. 60.
61. Hidalgo T, Verrall M, Beinlich A, Kuhar L, Putnis A (2020) Replacement reactions of copper sulphides at moderate temperature in acidic solutions, *Ore Geology Reviews*, 123, 103569.
62. Hidalgo T, McDonald R, Beinlich A, Kuhar L, Putnis A (2022) Comparative analysis of copper dissolution and mineral transformations in coarse chalcopyrite for different oxidant/lixiviant systems at elevated temperature (110 °C and 170 °C), *Hydrometallurgy*, 207, 105700.
63. Hidalgo T, Kuhar L, Beinlich A, Putnis A (2020) Effect of multistage solution–mineral contact in in-situ recovery for low-grade natural copper samples: Extraction, acid consumption, gangue-mineral changes and precipitation, *Minerals Engineering*, 159, 106616.
64. Kuhar L, Godel B, Hidalgo T, Evans A, Verrall M, Beinlich A, Rogers K (2020), High-resolution X-ray computed tomography study of coarse leached particles for in-situ recovery applications, *Proceedings of the ALTA ISR Conference 2020, Perth, Western Australia*.